RESEARCH ARTICLE

Reduction of Neuronal Intranuclear Rodlets Immunoreactive for Tubulin and Glucocorticoid Receptor in Alzheimer's Disease

John M. Woulfe[1]; Robert Hammond[2,3,4]; Bryan Richardson[5]; Danushan Sooriabalan[3]; William Parks[1]; Peter Rippstein[1]; David G. Munoz[3,4,6]

[1] Department of Pathology and Laboratory Medicine, The University of Ottawa, The Ottawa Hospital and The Ottawa Health Research Institute, Ontario, Canada.
[2] The Lawson Research Institute, London, Ontario, Canada.
[3] Department of Pathology, The University of Western Ontario, London, Canada.
[4] Department of Clinical Neurological Sciences, The University of Western Ontario, London, Canada.
[5] Department of Obstetrics and Gynecology, The University of Western Ontario, London, Canada.
[6] Servicio de Neurologia, "Doce de Octubre" Hospital, Madrid, Spain.

Neuronal intranuclear rodlets were described in normal brain over a century ago, but their functional significance and pathological relevance is unknown. Here, we show co-localization of tubulin and glucocorticoid receptor-like immunoreactivity in these intranuclear inclusions in human brain. In addition, we provide evidence for a massive reduction in their areal density in Alzheimer's disease brain, but not in another common neurodegenerative condition, dementia with Lewy bodies. The marked reduction of these inclusions in Alzheimer's disease may support the concept of a role for stress hormones in Alzheimer's pathogenesis.

Brain Pathol 2002;12:300-307.

Introduction

We recently documented the existence and described the topographic distribution of rod-shaped neuronal intranuclear inclusions, immunoreactive for the neuron-specific cytoskeletal protein class III β tubulin (C3βT), in the normal human brain (33). They display a widespread but anatomically selective distribution and are numerous in the basal forebrain, entorhinal cortex, temporal neocortex, hilum of the hippocampal dentate gyrus, substantia nigra, and inferior olivary nucleus. On light microscopic inspection, these inclusions are reminiscent of the intranuclear rodlets (INRs) described by the classical microscopists. The latter have been known to the light microscopists since the 1890s (18) and to electron microscopists since 1964 (29). They are included in the elegant descriptions of neuronal morphology by Santiago Ramon y Cajal based on his silver staining studies in a variety of species (5). INRs have been most often described in the nuclei of neuronal or paraneuronal cells. Although the rodlets are predominantly proteinaceous (14), the identity of their constituent proteins is unknown. Ultrastructurally, they consist of elongated intranuclear aggregates of dense filaments or more ordered paracrystalline arrays. Whether the tubulin immunoreactive inclusions we described correspond to these INRs remained to be determined.

Recently, one of us (RH) detected similar intranuclear structures in sections of fetal sheep brain which had been processed immunohistochemically for the detection of glucocorticoid receptor (GR) an intracellular receptor belonging to the superfamily of steroid-activated transcription factors. In the present study, we confirm GR-like immunoreactivity of tubulin-immunoreactive INRs. This finding is interesting in light of the significant influences which stress hormones, through GR activation, impose on brain structure and function (6, 16, 32), and potentially implicates INRs in steroid-mediated effects on the brain.

We were interested to determine whether there are disease-specific alterations in the density of INRs in AD brain relative to controls and those with other neurodegenerative disorders. To this end, we compared the areal density of INRs in the temporal cortex of brains among patients with AD, another common form of neurodegenerative dementia, dementia with Lewy bodies (DLB), and age-matched controls.

Materials and Methods

Tissue. Brain tissue was collected from our archive of formalin-fixed, paraffin-embedded blocks. A total of 46 human subjects was examined. A summary of the patient material studied here is found in Table 1. All autopsies were performed within 24 hours of the time of death. Subjects included 10 patients with neuropathologically-confirmed AD, 12 with DLB, and 24 age-matched control subjects in whom no evidence of dementia was found on review of the clinical chart.

Corresponding author:
Dr John Woulfe, Department of Pathology, The Ottawa Hospital, Civic Campus, 1053 Carling Avenue, Ottawa, Ontario, K1Y 4E9, Canada (e-mail: jwoulfe@ottawahospital.on.ca)

The control group was further subdivided on the basis of neuropathological findings into cases which displayed no diffuse or neuritic plaque formation on post-mortem light microscopic examination (6), those with abundant, exclusively diffuse cortical plaques (8), and those with additional, occasional neuritic plaques (10). The criteria outlined by The Consortium to Establish a Registry for Alzheimer's Disease (CERAD; 21) were employed to render a pathologic diagnosis of AD. In addition, we required neurofibrillary pathology at stages V or VI of Braak and Braak (3).

Immunohistochemistry. Single-labelling studies for the immunohistochemical localization of both C3βT and GR were performed using peroxidase immunohistochemistry on selected sections from AD and control brains. The primary antibody to C3βT (Sigma, St. Louis, MO, USA; Product # T8660, Clone SDL.310) used in the present study is a murine monoclonal antibody produced using a synthetic peptide corresponding to the carboxy-terminal sequence of human β tubulin isotype III. Single-labelling immunohistochemistry for the detection of C3βT using this antibody was carried out as reported previously (33). In control sections for the anti-tubulin antibody, primary antibody was replaced with an isotype specific (IgG 2b) control generated against an unrelated antigen.

The primary antibody to GR used in this study is an affinity-purified rabbit polyclonal antibody raised against a peptide mapping at the carboxy terminus of the α isoform of human GR (Santa Cruz Biotechnology, Santa Cruz, Calif; Product #sc-1002). Sections were subjected to antigen retrieval by microwaving for 5 minutes in 0.1 M citrate buffer, pH 5.6. Following immersion in 5% normal swine serum, primary antibody was applied at a dilution of 1:50 for 24 hours and visualization of bound antibody was achieved using the peroxidase-anti-peroxidase technique with diaminobenzidine as the chromogen. In control sections the antiserum was pre-absorbed with a synthetic peptide corresponding to the carboxy-terminal region of the α isoform of human GR (Santa Cruz Biotechnology, Santa Cruz, Calif; Product #SC-1002P).

For fluorescence double-labelling studies, formalin-fixed, paraffin-embedded blocks of mesial temporal lobe taken at the level of the lateral geniculate nucleus from randomly selected cases of AD and controls were cut into 4-μm thick sections and processed immunohistochemically for the simultaneous localization of C3βT and GR. Tissue was subjected to antigen retrieval by microwaving for 5 minutes in 0.1 M citrate buffer, pH 5.6, immersed in 5% normal goat serum for 20 minutes, then incubated in a cocktail containing the polyclonal anti-GR antibody diluted 1:50 and the murine monoclonal anti-C3βT antibody diluted 1:100. Following rinsing in phosphate buffer, the sections were incubated in a cocktail containing goat anti-rabbit Alexafluor 594 and goat anti-mouse Alexafluor 488 secondary antisera (Molecular Probes; Eugene, Ore) both diluted 1:100. In controls for double-labelling method specificity, one of each of the primary antibodies was omitted. Double-labelled sections were examined using confocal laser scanning microscopy. Images were collected with a Bio-Rad MRC 1024 confocal system on an Olympus IX 70 microscope. A 1.4 numerical aperture plan apochromat objective was used. The excitation of the green and red dyes was with laser light at 488 and 594 nm. The intensities of the 2 excitation sources could be independently controlled. This permits the selection of a ratio between the intensities to prevent cross talk between the 2 channels.

Category	N	Gender	Age Range	Mean Age
CONTROL	24	14M/10F	65-90	74.9
No plaques	*6*	*6M/0F*	*69-77*	*72.3*
Diffuse plaques	*8*	*4M/4F*	*65-90*	*75.8*
Neuritic	*10*	*4M/6F*	*67-84*	*75.8*
AD	10	3M/7F	67-87	79.9
DLB	12	10M/2F	69-93	78.2

Table 1. Age and gender profile of cases analyzed for INR counts.

Quantitation of INRs. For quantitative analysis of INRs in AD, DLB, and control brains, formalin-fixed, paraffin-embedded blocks of mesial temporal lobe from the cases listed in Table 1 taken at the level of the lateral geniculate nucleus, as well as blocks from the medulla, were cut into 6-μm thick sections and processed immunohistochemically for the demonstration of C3βT as described previously (33). To quantitate inclusions, sections were counted manually, in a blinded and random fashion, using an ocular reticule and a Leitz Dialux microscope. Five non-overlapping strips of cortex extending from the pial surface to the corticomedullary junction of the cortex lining the lateral bank of the collateral sulcus were counted under the 10× objective. The values for each case were expressed as the mean number of INRs per mm^2 .

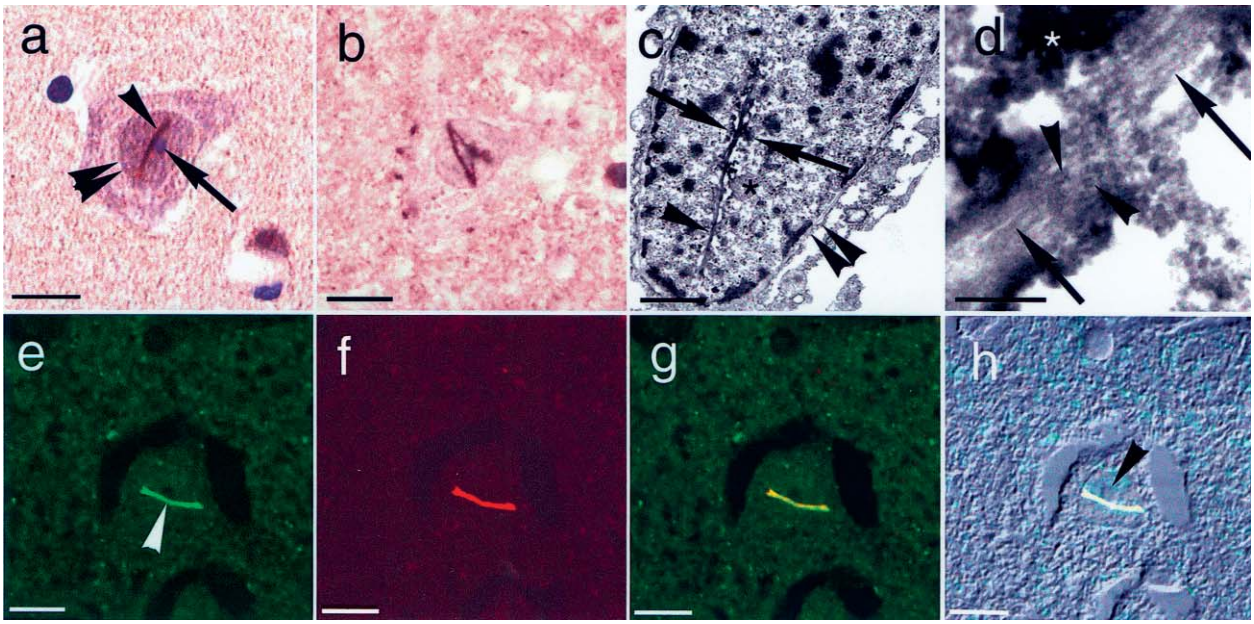

Figure 1. INRs in normal brain. **a, b.** Light micrographs showing rod-shaped INRs immunoreactive for C3βT (**a**) and GR (**b**) in neurons of the temporal neocortex of control brain. Double arrowheads in (**a**) indicate the nuclear membrane. Note the proximity of the rod-shaped intranuclear inclusion (single arrowhead in a) to the nucleolus (arrow in **a**). **c.** Electron micrograph showing a rod-shaped neuronal INR (arrowhead). Double arrowheads indicate the nuclear membrane. The rodlet is surrounded by dense, floccular DAB reaction product (arrows). Note the proximity of the INR to the nucleolus (asterisk). Bar = 2.5 μm. **d.** Higher magnification electron micrograph showing INR filaments in longitudinal (arrows) and transverse (arrowheads) planes of section. Note the circular appearance of the individual fibrils in the latter. The asterisk indicates the DAB reaction product. Bar = 180 nm. **e-h.** Confocal laser scanning microscopic images showing a rod-shaped neuronal intranuclear inclusion (arrowhead in **e**) double-immunostained for C3βT (**e**; green) and GR (**f**; red) in the temporal neocortex. The merged image is shown in g. h shows the merged image superimposed on the transmitted light differential interference contrast image. Note the proximity of the inclusion to the nucleolus (arrowhead). Bars = 10 μm.

Using an identical procedure, neurons were counted in haematoxylin and eosin stained sections adjacent to those processed immunohistochemically. Results were expressed as neurons/mm^2, then number of INRs/neuron. For this analysis, tissue suitable for both neuronal counts and INR counts was available from 22 controls, 9 AD cases, and 11 DLB cases.

Electron microscopy. Tissue was prepared for electron microscopy using the "pop-off" technique. Slides containing sections of control brain immunostained for C3βT or GR using peroxidase immunohistochemistry were examined under the light microscope. Areas containing INRs were marked and the slides were de-coverslipped in xylene, de-paraffinized, and processed routinely for electron microscopy. Capsules containing Spurr-resin were applied to the marked region on the slide-mounted section and polymerized for 24 hours at 80ºC. Following polymerization, part of the section was "popped-off" from the slide, trimmed, cut at 600-μm thickness onto copper grids, stained with uranyl acetate, and lead citrate, and examined using a Hitachi 7100 transmission electron microscope.

Results and Discussion

Relationship between class III β tubulin-immunoreactive neuronal intranuclear inclusions and intranuclear rodlets. In order to determine whether these C3βT-immunoreactive inclusions represented the INRs of the classical microscopists, sections of human post-mortem temporal lobe were immunostained for C3βT and examined by light and electron microscopy. Intensely C3βT-immunoreactive inclusions were identified in a topographical pattern of distribution identical to that reported previously (33). Specifically, they were present in the temporal neocortex where they were concentrated in larger neurons in layers III and V. Here, they displayed a variety of shapes including rod-shaped (Figure 1a), crystalloid, and dot-like. Rare neuronal nuclei contained two distinct inclusions. Occasional rod-shaped inclusions displayed

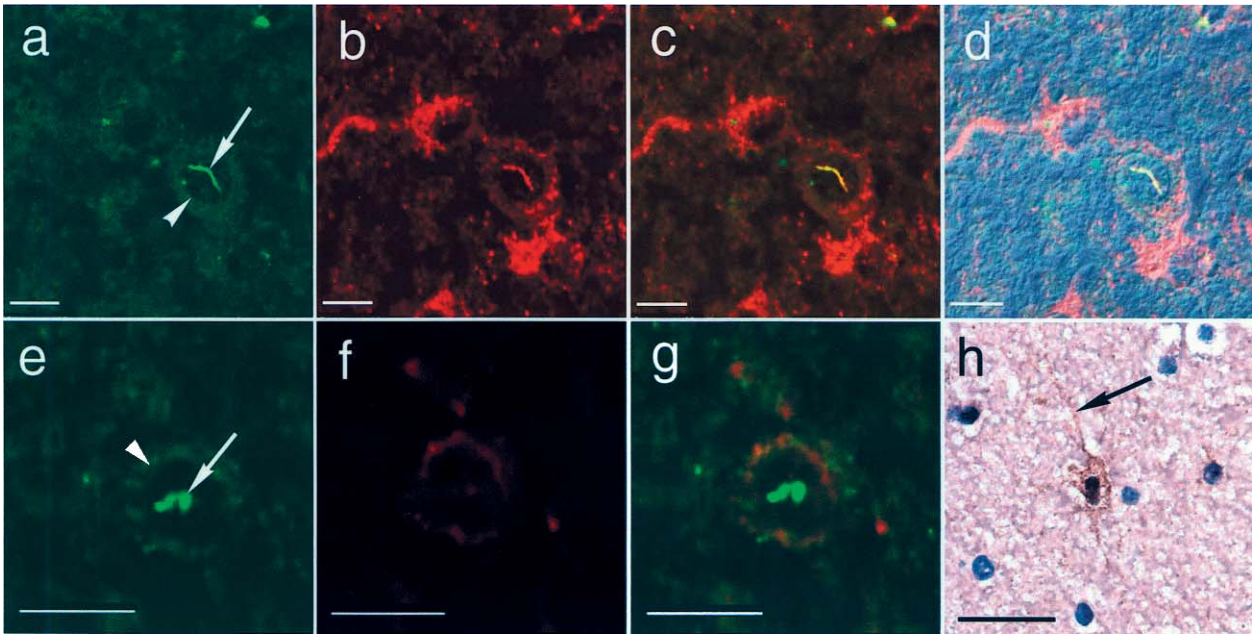

Figure 2. INRs in AD brain. **a-d.** Confocal laser scanning microscopic images showing a curved INR (arrow in **a**) double-immunostained for C3βT (**a**; green) and GR (**b**; red) in the temporal neocortex of AD brain. The arrowhead in (**a**) indicates the nuclear membrane. The merged image is shown in **c**. **d** shows the merged image superimposed on the transmitted light differential interference contrast images. **e-g.** Confocal scanning laser microscopic images showing an irregular neuronal intranuclear inclusion (arrow in **e**) in the temporal cortex of AD brain immunoreactive for C3βT (**e**; green), but not GR (**f**; red). The arrowhead in (**e**) indicates the nuclear membrane. The merged image is shown in **g**. **h.** Light micrograph showing light cytoplasmic GR-like immunoreactivity in the perikaryon and processes (arrow) of an astrocyte in the subcortical white matter of AD temporal cortex (immunoperoxidase). Bars = 10 μm.

branching or a complex "folded" appearance (see Figure 1b). Inclusions were also prevalent in the hilum of the dentate gyrus. The hippocampal CA1-CA3 subregions and subiculum displayed only rare inclusions. No labelling was seen in control sections in which the primary antibody was replaced with an isotype specific (IgG 2b) control generated against an unrelated antigen. The inclusions conformed in their ultrastructural appearance to the INRs described in previous morphological studies (Figure 1c, d). Specifically, in sections of temporal cortex, the INRs appeared as spindle- or rod-shaped structures of an indeterminate length surrounded by coarse deposits of electron-dense diaminobenzidine reaction product. They were typically composed of parallel arrays of tightly-packed fibrils. At higher magnification, individual nuclear fibrils appeared as tubules, displaying a "doublet" appearance in longitudinal planes of section and a circular profile in cross-section (Figure 1d). Each tubular fibril had an external diameter of between 12.8 and 16.6 nm. No "paracrystalline" or "crystalline" forms were observed. We concluded that C3βT immunoreactive INRs correspond to at least a subset of the intranuclear inclusions described by the classical microscopists. Morphological descriptions of the latter include "paracrystalline" and filamentous forms. Filamentous INRs formed by tubular filaments, similar to those reported here, have been observed in neurons from sympathetic ganglia (28). We conclude that the C3βT-immunoreactive intranuclear inclusions correspond to at least a subset of the INRs described in previous morphological studies.

Glucocorticoid receptor-like immunoreactivity of intranuclear rodlets. Immunohistochemical localization of GR in sections of human temporal cortex using an affinity-purified rabbit polyclonal antibody raised against the α isoform of human GR revealed neuronal intranuclear inclusions displaying a morphology and topographic distribution identical to that described for C3βT-positive INRs (Figure 1b). This immunoreactivity was completely abolished by pre-adsorption of the antibody with the synthetic peptide against which the polyclonal antiserum was generated. However, pending biochemical confirmation of the existence of the GR protein in INRs, the GR immunoreactivity we demon-

strated will heretofore be referred to as "GR-like immunoreactivity."

In order to determine whether INRs displayed immunoreactivity for both C3βT and GR, fluorescence double-labelling immunohistochemistry was performed on sections of mesial temporal lobe from brains of normal control cases as well as selected cases with Alzheimer's disease. Confocal laser scanning microspcopic imaging confirmed an intimate co-localization of C3βT and GR-like immunoreactivities in INRs in control brain (Figure 1e-h). No inclusions stained exclusively for either C3βT or GR in control brain. In AD brain, the vast majority of INRs were also immunoreactive for both antibodies (Figure 2a-d). However, in many of the inclusions in AD brain, the GR-like immunoreactivity appeared qualitatively weaker than that for tubulin, and very rare inclusions were labeled for C3βT only (Figure 2e-g). The factors underlying this dissociation are uncertain. It certainly indicates that the two antibodies are recognizing separate antigens within INRs. Whether this apparent reduction in GR-like staining has any pathogenetic relevance awaits further studies. In control sections, omission of either primary antibody resulted in absence of staining for that antigen. In addition, there were C3βT positive structures (neurites) that were negative for GR. Conversely, in AD brain, the cortical neuropil contained GR-positive threadlike structures that were negative for tubulin. In AD brain, reactive astrocytes showed light cytoplasmic GR-like immunostaining (Figure 2h). These were tubulin negative.

The co-localization of C3βT and GR-like immunoreactivity in the neuronal nucleus demonstrated in the present study is consistent with previous studies documenting GR-tubulin interactions in the perikaryal compartment. Co-localization of GR with tubulin has been documented extensively in both biochemical and immunohistochemical studies. With respect to the former, tubulin has been detected in purified preparations of activated GR (1). Conversely, activated GR has been found to associate with a cytoskeletal protein complex containing tubulin (26). In immunohistochemical studies, GR has been co-localized with microtubules in fixed mammalian cells (1). In gingival fibroblasts, there is co-localization of GR and tubulin in vinblastine-induced paracrystals (1). In the context of the present study, it is interesting that these predominantly cytoplasmic tubulin-GR immunoreactive paracrystals were sometimes localized within the fibroblast nucleus.

The functional significance of neuronal INRs has remained enigmatic. Some studies have related their expression to neuronal activity (18, 27). The identity of the GR-immunoreactive antigen within INRs remains to be determined. In the context of the previous evidence outlined above for the existence of GR-tubulin complexes, it is conceivable that it represents functional GR or a GR-related protein. Such an intranuclear interaction could indicate an important role for INRs in stress hormone influences on the brain. Low to moderate levels of glucocorticoids promote synaptic plasticity, long term potentiation, and learning and memory. Specifically, GR activation is involved in consolidation of learned information (23). In excess, they have detrimental consequences. The latter have been studied most extensively in the hippocampus where excess corticosteroid levels for prolonged periods of time lead to morphological changes, particularly in CA3 hippocampal neurons with atrophy of distal dendrites (32). Glucocorticoid hormones influence both neuronal apoptosis (4) and neurogenesis (6) in the dentate gyrus. These cellular alterations have cognitive and behavioural correlates. Indeed, hypercortisolemia or stress impair memory and learning (7, 16).

In light of these findings, it is not surprising that aberrations in the hypothalamo-pituitary-adrenal axis and stress hormone systems have been demonstrated in AD (8, 11, 22, 31). Patients with AD display increased concentrations of cortisol in plasma and urine and an increased plasma cortisol response to stress (8, 22). In mild cognitive decline and AD, the extent of hippocampal atrophy correlates well with plasma glucocorticoid levels (8, 22, 31). Increased stress hormones in AD may lower the threshold for neuronal degeneration in AD (31). Indeed, glucocorticoids can enhance the oxidative damage induced by β-amyloid protein and glutamate in cultured hippocampal neurons, perhaps by blocking endogenous NF-κB-driven cell defense programs (2). Finally, there is a relationship between cerebrospinal fluid cortisol levels in AD and apolipoprotein E genotype (25).

Reduction of intranuclear rodlets in Alzheimer's disease. We compared the density of C3βT-immunoreactive INRs among brains of patients with AD, controls, and DLB. A summary of the patient material studied is shown in Table 1. Systematic counts of C3βT-immunoreactive INRs in the temporal cortex of AD, DLB, and control cases revealed a greater than 95% reduction in the areal density of INRs in AD relative to control and DLB subjects (Figure 3). Because the distributions of values for INR counts per mm^2 of cerebral cortex and for INRs per neuron did not conform to a normal distribution, we employed non-parametric

tests for group comparisons and direct comparisons. The Kruskal-Wallis one way analysis of variance on ranks with respect to the areal density of INRs in the temporal cortex among AD (mean = 0.133/mm^2), DLB (3.302/mm^2), and control subjects (4.556/mm^2) revealed a highly significant difference ($p<0.001$; Figure 3a). An all pairwise multiple comparison procedures analysis (Dunn's method) revealed significant differences between AD and control groups as well as AD and DLB groups ($p<0.05$, respectively) but no significant differences between control and DLB groups. In a separate analysis, there were no significant differences among the 3 control subgroups, namely; those without plaques, those with diffuse plaques, and those with neuritic plaques (Figure 3a). Interestingly however, there was considerable variability in the density of inclusions among DLB cases (Figure 3b). Upon review, it became clear that the cases with reduced INR counts were those harbouring additional AD pathology in the form of abundant neuritic plaques (data not shown).

In order to determine whether the significant deficit of INRs demonstrated in AD brain was attributable to discrepancies in cortical neuronal density between AD and the other groups, neuronal counts were performed in sections adjacent to those processed immunohistochemically and inclusion counts were translated into mean number of INRs per neuron. This analysis did reveal a significant reduction in neuronal density by approximately 21% in AD (436 neurons/mm^2) and 12% in DLB (486 neurons/mm^2) relative to controls (553 neurons/mm^2; $p<0.05$). This 21% reduction corresponds well with previous estimates of neuronal loss in AD neocortex (30; see below). However, it is miniscule relative to the reduction in INR density. Indeed Kruskal-Wallis one way analysis of variance on ranks revealed a significant difference with respect to number of INRs per neuron among the control (mean = 8.20×10^{-3}), DLB (7.20×10^{-3}), and AD (0.30×10^{-3}) groups ($p<0.001$; Figures 3b, c). Direct comparison of the AD and DLB groups using the all pairwise multiple comparison procedures test (Dunn's method) disclosed a statistically significant difference with respect to number of rods per neuron between the AD and control groups, as well as the AD and DLB groups ($p<0.05$, respectively) but not between control and DLB cases.

Relative to other structure-specific deficits described in the brains of AD patients, the reduction in INRs described in the present study is profound. For example, depending on disease severity, neuronal loss in AD varies from 20 to 40% in the neocortex (30) and approximates 35% in the nucleus basalis of Meynert

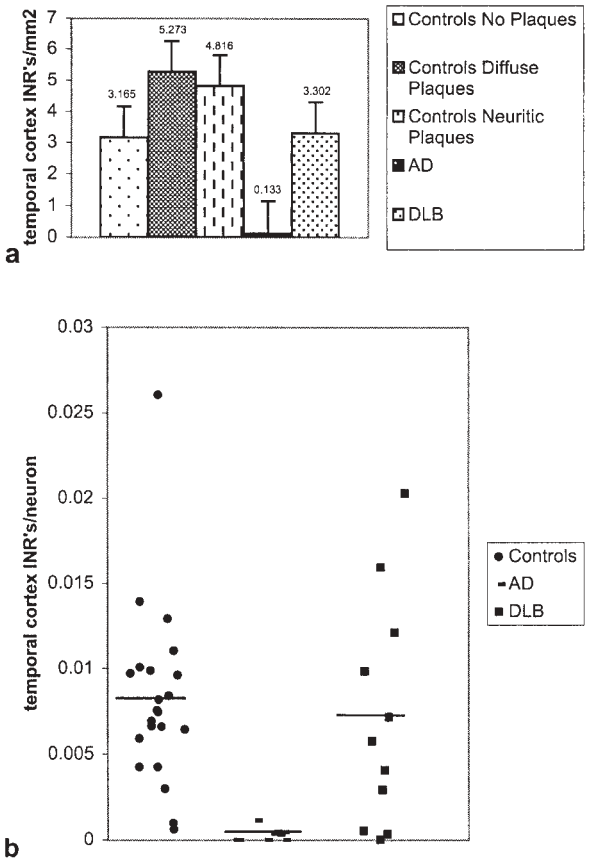

Figure 3. INRs are reduced in AD. **a.** Bar graph comparing mean number of INRs per mm^2 in temporal cortex of controls (without plaques, with diffuse plaques, and with neuritic plaques), patients with AD, and patients with DLB. **b.** Scatterplot of INRs per neuron among control, AD, and DLB cases.

(24), the major source of cholinergic innervation of the cerebral cortex. Even in advanced cases, estimates of synaptic loss are 20 to 60% in frontal cortex, 10 to 30% in temporal and parietal cortex, and 30% in the nucleus basalis (19). By contrast, INRs are reduced by approximately 95%, to approximately 10% of their normal density in all cases of AD we have studied. INRs are not reduced in DLB. The substrate of dementia in up to 20% of cases, DLB is characterized pathologically by the presence of intraneuronal Lewy bodies in neocortical, limbic, and subcortical regions. Whether DLB represents a variant of AD or is a distinct entity has been a matter of considerable debate due to the presence of both types of pathology in many cases. Distinguishing or unifying AD and DLB on genetic grounds has also been difficult. ApoE genotyping has yielded inconsistent results. The wide discrepancy between AD and DLB with respect to INR density supports the separation of

these diseases as distinct entities and indicates that INR loss is not a non-specific effect of dementia or brain atrophy.

The factors underlying this reduction of INRs in AD cortex remain to be defined. There are several possible interpretations of this phenomenon. For example, it is conceivable that INRs represent a morphological marker of selective neuronal vulnerability in AD. Neuronal loss in AD is not random. Neurons expressing non-phosphorylated neurofilament protein show a marked and selective depletion in AD brain, the severity of which approaches that of INRs demonstrated in the present study (12). The factors conferring this selective vulnerability are unknown. In this context, it is interesting that, in normal cortex, neurofilament-positive neurons show a laminar pattern of distribution identical to that described for INRs (12). Immunohistochemical double-labelling studies are underway to determine whether INRs are selectively localized to the vulnerable neurofilament-positive neurons.

Alternatively, it is possible that INR reduction accompanies, or even underlies, other abnormalities in nuclear morphology and function that have been demonstrated in AD. INRs show a consistent relationship to the nucleolus and/or granulofibrillary (accessory) bodies, both of which are involved in gene transcription (9, 15, 20). Reduction of nucleolar volume, neuronal RNA content and nuclear transcription have been demonstrated in AD (10, 13, 17). INR reduction may therefore represent an additional manifestation of these nuclear perturbations.

Conclusion

The massive reduction in the areal density of INRs in AD, but not DLB, supports the concept that these 2 neurodegenerative disorders are pathologically distinct entities. INRs may represent a morphological marker of selective neuronal vulnerability in AD. Their reduction in AD may be related to other nuclear abnormalities, both structural and functional, that have been described in AD brain. Finally, the GR-like immunoreactivity demonstrated in INRs in the present study suggests that these structures may have a role in stress-hormone mediated influences on the brain and their involvement in AD pathogenesis.

Acknowledgments

The authors wish to acknowledge the excellent technical assistance of Mr Roy Taylor and Mr Andrew Ridsdale. This study was funded by The Hamilton Health Sciences Corporation, The Ottawa Hospital, and “Fondo de Investigacion del SNS” of Spain (Expediente 98/3157).

References

1. Akner G, Sundqvist K-G, Denis M, Wikstrom A-C, Gustafsson JA (1990) Immunocytochemical localization of glucocorticoid receptor in human gingival fibroblasts and evidence for a colocalization of glucocorticoid receptor with cytoplasmic microtubules. *Eur J Cell Biol* 53:390-401.
2. Behl C (1998) Effects of glucocorticoids on oxidative stress-induced hippocampal cell death: implications for the pathogenesis of Alzheimer’s disease. *Exp Gerontol* 33:689-696.
3. Braak H, Braak E (1995) Staging of Alzheimer's disease-related neurofibrillary changes. *Neurobiol Aging* 16:271-278.
4. Bye N, Nichols NR (1998) Adrenalectomy-induced apoptosis and glial responsiveness during aging. *Neuroreport* 20:1179-1184.
5. Cajal RYS (1911) Histologie du systeme nerveux de l’homme et des vertebres. II, Maloine: Paris.
6. Cameron HA, Gould E (1994) Adult neurogenesis is regulated by adrenal steroids in the dentate gyrus. *Neuroscience* 61:203-209.
7. Conrad CD, Galea LA, Kuroda Y, McEwen BS (1996) Chronic stress impairs rat spatial memory on the Y maze and this effect is blocked by tianeptine pretreatment. *Behav Neurosci* 110:1321-1334.
8. Davis KL, Davis BM, Greenwald BS, Mohs RC, Mathe AA, Johns CA, Horvath, TB (1986) Cortisol and Alzheimer’s disease Ibasal studies. *Am J Psychiatr* 143:300-305.
9. Feldman ML, Peters A (1972) Intranuclear rods and sheets in rat cochlear nucleus. *J Neurocytol* 1:109-127.
10. Harrison PJ, Barton AJ, Najlerahim A, McDonald B, Pearson RC (1991) Regional and neuronal reductions of polyadenylated messenger RNA in Alzheimer’s disease. *Psychol Med* 21:855-866.
11. Hartmann A, Velhuis JD, Deuschle M, Standhardt H, Heuser I (1997) Twenty-four hour cortisol release profiles in patients with Alzheimer’s and Parkinson’s disease: ultradian secretory pulsatility and clinical variation. *Neurobiol Aging* 18:285-289.
12. Hof PR, Cox K, Morrison JH (1990) Quantitative analysis of a vulnerable subset of pyramidal neurons in Alzheimer’s disease: I. Superior frontal and inferior temporal cortex. *J Comp Neurol* 301:44-54.
13. Husseman JW, Hallows JL, Bregman DB, Leverenz JB, Nochlin D, Jin L-W, Vincent I (2001) Hyperphosphorylation of RNA polymerase II and reduced neuronal RNA levels precede neurofibrillary tangles in Alzheimer disease. *J Neuropathol Exp Neurol* 60:1219-1232.
14. Kim S, Masurovsky E, Benitez H, Murray M (1970) Histochemical studies of the intranuclear rodlet in neurons of the chicken sympathetic and sensory ganglia. *Histochemie* 24:33-40.

15. Lafarga M, Berciano MT, Andres MA (1993) Protein-synthesis inhibition induces perichromatin granule accumulation and intranuclear rodlet formation in osmotically stimulated supraoptic neurons. *Anat Embryol* 187:363-369.
16. Lupien SJ, McEwen BS (1997) The acute effects of corticosteroids on cognition: integration of animal and human model studies. *Brain Res Rev* 24:1-27.
17. Mann DM, Yates PO, Barton CM (1977) Cytomorphometric mapping of neuronal changes in senile dementia. *J Neurol Neurosurg Psychiatry* 40:299-302.
18. Mann G (1894) Histological changes induced in sympathetic, motor, and sensory nerve cells by functional activity. *Anat Physiol* 29:100-108.
19. Masurovsky EB, Benitez HH, Kim S-U, Murray MR (1970) Origin, development, and nature of intranuclear rodlets and associated bodies in chicken sympathetic neurons. *J Cell Biol* 44:172-191.
20. Masliah E, LiCastro F (2000) Neuronal and synaptic loss, reactive gliosis, microglial response, and induction of complement cascade in Alzheimer's disease. In: *Neurodegenerative Dementias*, Clark CM, Trojanowski JQ (eds.), Chapter 9, pp.131-146, McGraw-Hill: New York.
21. Mirra SS, Heyman A, McKeel D, Sumi SM, Crain BJ, Brownlee LM, Vogel FS, Hughes JP, van Belle G, Berg L (1991) The Consortium to Establish a Registry for Alzheimer's Disease (CERAD). Part II. Standardization of the neuropathologic assessment of Alzheimer's disease. *Neurology* 41:479-486.
22. Nasman B, Olsson T, Fagerlund M, Eriksson S, Viitanen M, Carlstrom K (1996) Blunted adrenocorticotropin and increased adrenal steroid response to human corticotropin-releasing hormone in Alzheimer's disease. *Biol Psychiatry* 39:311-318.
23. Oitzl MS, de Kloet ER (1992) Selective corticosteroid antagonists modulate specific aspects of spatial orientation learning. *Behav Neurosci* 106:62-71.
24. Perry RH, Candy JM, Perry EK, Irving D, Blessed G, Fairbairn AF, Tomlinson B.E. (1982) Extensive loss of choline acetyltransferase activity is not reflected by neuronal loss in the nucleus basalis of Meynert in Alzheimer's disease. *Neurosci Lett* 33:311-315.
25. Peskind ER, Wilkinson CW, Petrie EC, Schellenber GD, Raskind MA (2001) Increased csf cortisol in AD is a function of ApoE genotype. *Neurology* 56:1094-1098.
26. Scherrer LC, Pratt WB (1992) Association of transformed glucocorticoid receptor with a cytoskeletal protein complex. *J Steroid Biochem Molec Biol* 41:719-721.
27. Seite R, Mei N, Villet-Luciani J (1973) Effect of electrical stimulation on nuclear microfilaments and microtubules of sympathetic neurons submitted to cycloheximide. *Brain Res* 50:419-423.
28. Seite R, Vuillet-Luciani J, Zerbib R, Cataldo C, Escaig J, Pebusque MJ, Autillo-Touati A (1979) Thee-dimensional organization of tubular and filamentous nuclear inclusions and associated structures in sympathetic neurons as revealed by serial sections and tilting experiments. *J Ultrastruct Res* 69:211-231.
29. Siegesmund K, Dutta C, Fox C (1964) The ultrastructure of the intranuclear rodlet in certain nerve cells. *J Anat* 98:93-97.
30. Terry RD, Peck A, De Teresa R, Schechter R, Horoupian HD (1981) Some morphometric aspects of the brain in senile dementia of the Alzheimer's type. *Ann Neurol* 10:184-192.
31. Weiner MF, Vobach S, Olsson K, Svetlik D, Risser RC (1997) Cortisol secretion and Alzheimer's disease progression. *Biol Psychiatry* 42:1030-1038.
32. Woolley CS, Gould E, McEwen BS (1990) Exposure to excess glucocorticoids alters dendritic morphology of adult hippocampal pyramidal neurons. *Brain Res* 531:225-231.
33. Woulfe J, Munoz D (2000) Tubulin immunoreactive neuronal intranuclear inclusions in the human brain. *Neuropathol Appl Neurobiol* 26:161-171.